A computational study of some possible factors associated with Melt Eruption Events

Will Schreiber[1] and John Kuo[2]

ABSTRACT

The current paper describes a computer model designed to analyze the moisture transport in the unmelted, porous soil neighboring a convecting melt. The time-dependent fluid and heat flow in the soil melt is simulated implicitly using the SIMPLE method generalized to predict viscous fluid motion and heat transfer on boundary-fitted, non-orthogonal coordinates which adapt with time. TOUGH2, a general-purpose computer code for multiphase fluid and heat flow developed by K. Pruess at Lawrence Berkeley Laboratory, has been modified for use on time-adaptive, boundary-fitted coordinates to predict heat transfer, moisture and air transport, and pressure distribution in the porous, unmelted soil. The soil melt model is coupled with the modified TOUGH2 model via an interface (moving boundary) whose shape is determined implicitly with the progression of time.

The computer model's utility is demonstrated in the present study with a special two-dimensional study. A soil initially at 20°C and partially saturated with either a 0.2 or 0.5 relative liquid saturation is contained in a box two meters wide by ten meters high with impermeable bottom and sides. The upper surface of the soil is exposed to a 20°C atmosphere to which vapor and air can escape. Computation begins when the soil, which melts at 1700°C is heated from one side (maintained at constant temperatures ranging from 1700°C to 4000°C). Heat from the hot wall causes the melt to circulate in such a way that the melt interface grows more rapidly at the top of the box than at the bottom. As the upper portion of the melt approaches the impermeable wall it creates a bottleneck for moisture release from the soil's lower regions. The pressure history of the trapped moisture is examined as a means for predicting the potential for moisture penetration into the melt. The melt's interface movement and moisture transport in the unmelted, porous soil are also examined.

INTRODUCTION

The *In Situ* Vitrification (ISV) process offers an economical and relatively uncomplicated means of remediating buried contaminants such as nuclear and toxic chemical wastes. The ISV process consists of melting the contaminated soil with electrodes or plasma torches while capturing off-gases in a hood that covers the treatment site. After the designated volume of contaminated soil, up to ten meters in diameter, has been melted, it is subsequently allowed to solidify into an impervious glass. The glassified contaminated soil is, for all practical purposes, entirely impervious to ground water and can be safely left on site.

While the ISV process has been used successfully by both government and commercial interests to remediate numerous contaminated sites, there have been problems in several isolated instances in the form of Melt Eruption Events (MEE). During an MEE, the melt erupts to spatter equipment in the off-gas hood and to release pressurized gas products into the atmosphere. One likely scenario postulated for these problems is that soil moisture becomes trapped between the encroaching melt front and an impervious surface. Once the soil vapor has been effectively sealed off from any escape route, it pressurizes rapidly to the point where it is forced into the melt. Having broached the melt, the gas is energized and leads to an MEE. It is generally agreed that better site characterization in concert with an improved understanding of the interaction of melting soil with moisture transport in the native soil are needed to improve the safety of the ISV process. Conceptual models for this phenomenon have been formulated, and one of these models has been simulated previously using thermal hydraulic numerical codes (Roberts et al. 1992, Schreiber 1996a,b).

The current paper describes a computational method for examining the effect of melt movement on moisture transport and pressure build-up in the surrounding soil.

At its current stage of development, the model makes two major restricting assumptions.

1. Melt viscosity is considered constant.
2. Density difference between the porous soil and the melted soil is ignored; consequently, the fluid melt occupies the same volume as the porous soil it has displaced.

Both of these restrictions will admittedly affect the model's predictions but can be addressed in a more elaborate model.

---

[1] Associate Professor, Mechanical Engineering Department, The University of Alabama, PO Box 870276, Tuscaloosa, AL 35487

[2] Research Engineer, ADT Engineering, Inc., Flint Michigan

MATHEMATICAL MODELS

Three models are combined for the purposes of prediction described in the abstract and introduction sections. All three models are generalized for use on a non-orthogonal, boundary-fitted grid that adapts to a growing melt. A CFD model of the melt (Kuo and Schreiber, 1994) is coupled, via a moving interface model, to a general-purpose computer code, TOUGH2 developed by Pruess (1985,1986), for multiphase fluid and heat flow in a porous medium. The CFD model has been developed to predict fluid flow and heat transfer of a viscous fluid, the melt, on a non-orthogonal, boundary-fitted grid that adapts to a growing melt. The TOUGH2 code has been modified to enable its use for modeling moisture, air, and heat transport in the unmelted soil on a similar time-dependent grid system that is congruent with the melt region. (See Figure 1.) The interface that separates the melted and unmelted regions is calculated in terms of a heat balance including latent heat of phase change. The calculation procedure for the interface is implicit in time so as to allow a reasonably large time step.

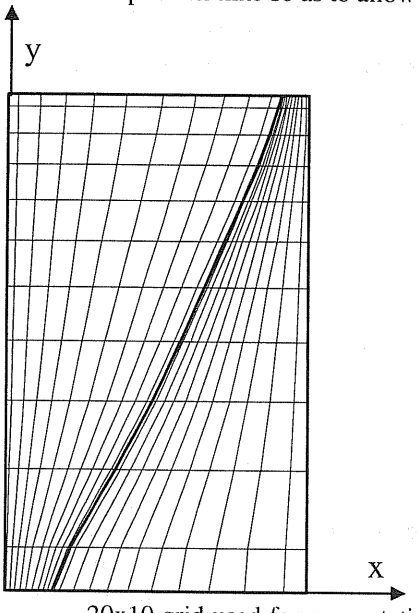

Figure 1. 20x10 grid used for computation. Grid to the left of the diagonally oriented, curved interface used by CFD melt code; grid to the right of the interface used by TOUGH2. Scale of picture is expanded by a factor of three in the horizontal (x) direction.

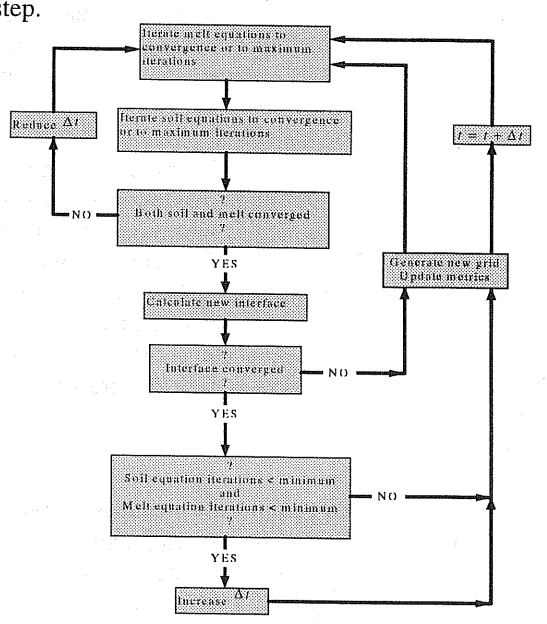

Figure 2. Flow chart for algorithm used to exact interface movement implicitly in time.

In TOUGH2, an integral equation describes the balance of M, the accumulation of internal energy or species, relative to a control volume, V_n.

$$\frac{d}{dt}\int_{V_n} M^{(\kappa)}\,dv = \oint (F^{(\kappa)}\cdot\hat{n}) + \int_{V_n} q^{(\kappa)}\,dv \qquad (1)$$

The term F is the flux of mass or heat, q is the source of mass or heat (per volume), t is time, and $\hat{n}$ is the direction normal and inward to a control volume surface. The superscript (κ) is the species index where: $\kappa = 1$: water, $\kappa = 2$: air, and $\kappa = 3$: heat.

Further formulas are described in reference 2 that define the storage, flux, and generation terms found in equation (1) for species transfer and for heat transfer as well as the constitutive equations needed to relate thermodynamic properties. The thermodynamic state of each control volume is described in the code in terms of the primary properties. Secondary properties are determined with constitutive equations as a function of the primary properties. After it is differenced implicitly in time, equation (1) may be expressed in terms of a residual

$$R_n^{(\kappa)k+1} = M_n^{(\kappa)k+1} - M_n^{(\kappa)k} - \frac{\Delta t}{V_n}\left(\sum_m A_m F_m^{(\kappa)k+1} + V_n q_n^{(\kappa)k+1}\right) = 0 \qquad (2)$$

where R is the numerical residual, A is the control volume interface area. The index n signifies the control volume, m indicated the neighboring control volume index, and k is the time step index.
The residual is minimized using the Newton-Raphson method to find the values at the k+1 time implicitly.

To predict transport in a static domain, TOUGH2 does not require that the control volumes be ordered in terms of a grid. Only the interface areas between the control volumes and the size of the control volumes need be provided as input data. In order to incorporate domain boundaries, which adapt with time; however, a grid system must be imposed since the time-dependent volume and interface areas of each control volume depend on the location of the moving interface boundary. In the current application of TOUGH2, the control volumes are mapped to an ordered two-dimensional coordinate system (referred to as the physical space, x-y) as pictured in figure 1. This non-orthogonal grid is further mapped to a rectangular grid (known as the computational space, $\xi - \eta$) through the use of geometric transformations (metrics). Thompson (1984) describes the grid generation and derives the geometric transformations needed to enact this mapping.

The TOUGH2 code has been modified to include the metrics needed to transform TOUGH2's differenced equations from physical to computational space. The input data for the code includes volumes and control volume interface areas of unit size plus the values of the metric coefficients needed to transform equations to conform to the boundary-fitted geometry. With each ensuing time step, the grid and metrics are recalculated to conform to the time-dependent interface boundary.

The equations that describe transport in the melt are also transformed to a computational space coordinate system in (ξ,η) where $\xi = \xi(x,y,t)$ and $\eta = \eta(x,y,t)$.

Transport of momentum (in which ϕ is the x or y component of velocity, U or V)

or **heat** (in which ϕ is the temperature, T)

$$\frac{\partial(\phi J)}{\partial t} + \frac{\partial}{\partial \xi}\left(U_r\phi - \alpha\Gamma\phi_\xi\right) + \frac{\partial}{\partial \eta}\left(V_r\phi - \gamma\Gamma\phi_\xi\right) = \frac{\partial}{\partial \xi}\left(-\beta\Gamma\phi_\eta\right) + \frac{\partial}{\partial \eta}\left(-\beta\Gamma\phi_\xi\right) + S_\phi \tag{3}$$

where: $$S_\phi = \frac{J}{\rho}\left[-\left(\frac{\partial p}{\partial n}\right)_\phi + B_\phi\right] \text{ for the momentum equations.} \tag{4}$$

The term B_ϕ is the body force, p is the dynamic pressure, Γ is the diffusivity, and ρ is the density. The term r indicates relative to grid velocity.

The geometric transformations found in the transport equation are:

$$J = x_\xi y_\eta - x_\eta y_\xi \tag{5}$$

$$\alpha = \left(x_\eta^2 + y_\eta^2\right)/J \tag{6}$$

$$\beta = \left(x_\xi x_\eta + y_\xi y_\eta\right)/J \tag{7}$$

$$\gamma = \left(x_\xi^2 + y_\xi^2\right)/J \tag{8}$$

Continuity

$$\frac{\partial U}{\partial \xi} + \frac{\partial V}{\partial \eta} = 0 \tag{9}$$

These equations are solved using a SIMPLE procedure modified to account for the non-orthogonal, time-dependent coordinate system. (Karki, 1986, and Kuo, 1994)

An equation is needed to determine the velocity $\tilde{U}_i$ of the isothermal interface. Latent heat, L_H, is required for melting the soil and is set equal to the difference of heat transferred from the melt to the interface and the heat transferred from the interface to the soil. This equation includes the assumption that the density of the porous soil is the same as that of the melt.

$$\frac{k_s\left(\alpha T_\xi\right)_s}{h_2} - \frac{k_{mt}\left(\alpha T_\xi\right)_{mt}}{h_2} = -J\rho L_H \tilde{U}_i \tag{10}$$

In this equation, the indices mt and s refer to the melt and the soil respectively, k is the conductivity, and L_H is the latent heat of soil matrix. The term, h_2, is a metric given by

$$h_2 = \sqrt{x_\eta^2 + y_\eta^2} \tag{11}$$

NUMERICAL PROCEDURE

The three computational models are all solved implicitly with time. A flow chart of the grand solution scheme is given in figure 2.

The TOUGH2 code was modified by including metrics for area and volume transformation as coefficients of the unit area and volume associated with each control volume. The effect of grid movement relative to the mass transport was included in the

computation. To account for the mass flow associated with grid movement, the volume metric for each control volume was modified in the residual equation (2) after each update of the grid and metrics. Including an advective heat flux proportional to the grid velocity modified heat conduction to include the effects of grid movement. While the characteristic time scales for the melt flow and porous flow codes were on the same order of magnitude, the time step size as depicted in figure 2 was mostly dictated by the melt flow equations.

RESULTS AND DISCUSSION

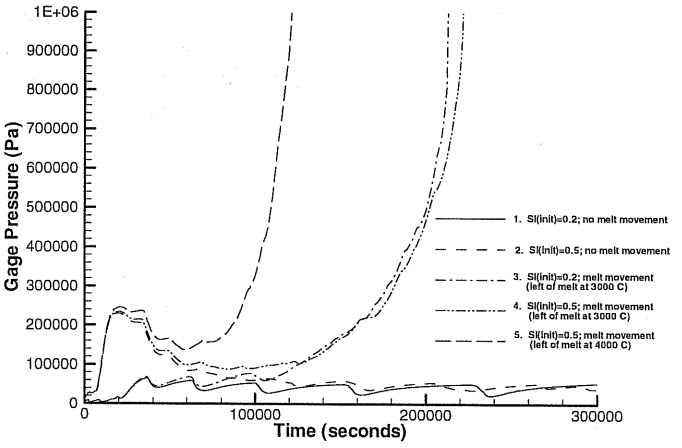

Figure 3. Pressure histories of porous soil at a point near bottom of melt.

The computer model's utility is demonstrated in the present study with a special two-dimensional case as described in the abstract. The soil simulated for this study has a soil grain density of $2900\,kg/m^3$, a porosity of 0.4, a permeability of 10^{-11} m^2, and a grain specific heat of $1.2\,kJ/kg\cdot K$. The soil's heat conductivity at saturation is $1.81\,W/m\cdot K$. The relative permeability function is described by the equations,

For the liquid water, $$k_{rl} = \sqrt{S^*}\left\{1-\left[1-\left(S^*\right)^{1/\lambda}\right]^{\lambda}\right\}^2 \tag{12}$$

For the water vapor, $$k_{rg} = 1 - k_{rl} \tag{13}$$

where $$S^* = \frac{S_l - 0.214}{1-0.214} \text{ and } \lambda = 0.63.$$

The capillary pressure function is given by,

$$P_{cap} = -P_o\left[\left(S^*\right)^{-1/\lambda} - 1\right]^{1-\lambda} \tag{9}$$

where $P_o = 18{,}250\,Pa$.

Case #	Rayleigh Number	Stefan Number	Initial Soil Liquid Saturation (S_l)
1	0	0	0.2
2	0	0	0.5
3	1.215×10^6	10.6	0.2
4	1.215×10^6	10.6	0.5
5	2.149×10^6	18.8	0.5

Table 1. Soil and melt data plus description of the five cases.

The melt properties are those of SiO_2 @ 1700°C and are not temperature-dependant in the current model. For brevity, the properties given in table 1 are given as non-dimensional in terms of the Rayleigh number (with a characteristic length of 2

meters and temperature difference between the isothermal wall and the 1700°C interface), the Stefan number, and the Prandtl number (which is 9.87×10^4 for all cases).

Depicted in figure 3 are histories of the pressure at a point in the porous soil located adjacent to the melt and the cavity's bottom. The pressure history curves exhibit some waviness that can be explained in terms of the numerical procedure. As the heat from the 1700°C interface is transferred to an adjacent saturated cell, the pressure and temperature of the cell rise slowly along the saturation curve. After the cell has dried out, the heat transferred from the cell, with its finite size and thermal inertia, to the next saturated cell will initially be less than the heat transferred from the interface to the first saturated cell. Steam generation in the next saturated cell is initially lower and the pressure drops until the dried out cell can reach a high enough temperature to cause the pressure to rise again in the next cell out.

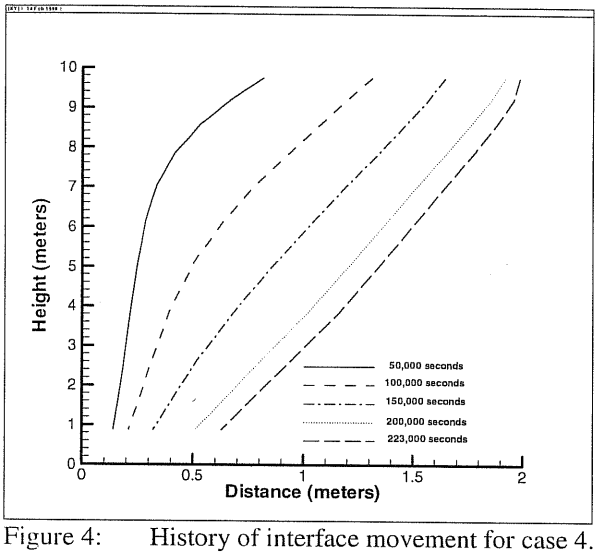

Figure 4: History of interface movement for case 4.

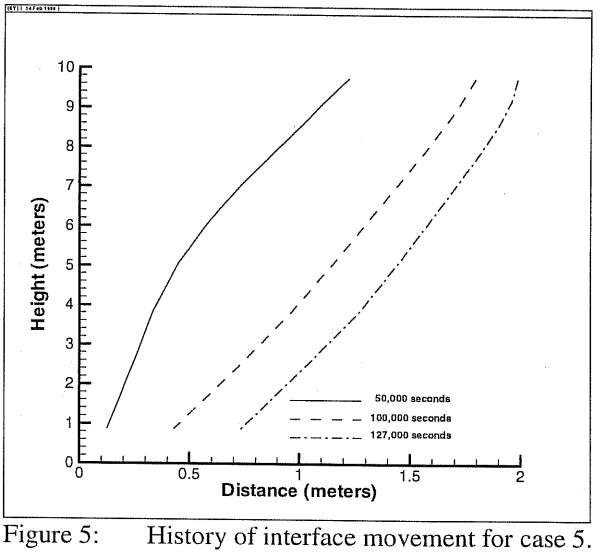

Figure 5: History of interface movement for case 5.

The pressure history curves for cases 1 and 2 remain well below one atmosphere. With no melt interface movement, the vapor path to the surface remains relatively unrestricted and pressure does not build up.

The pressure histories of cases 3 and 4 are similar. Initially, the pressures experience a rapid increase followed by a return to less than an atmosphere at about 100,000 seconds. Shortly after 100,000 seconds, the pressures for both cases experience a pronounced increase such that they exceed 10 atmospheres after a total time of 200,000 seconds. The pressure history curve for case 5 shows a similar pattern, except that the second pressure rise reaches 10 atmospheres shortly after 100,000 seconds.

The pressure histories can be explained by consideration of the melt interface histories seen in figures 4 and 5. Figure 4 illustrates the history of the interface movement for case 4. It is seen that the melt interface totally seals off the vapor release from the porous soil after 223,000 seconds. The initial increase in pressure for case 3 and 4 can be explained as result of the initial heat addition to the porous soil combined with melt movement. Until a dried out region is opened up for vapor to escape freely to the surface, the combination of rapid boil off near the interface and decreasing volume causes a temporary pressure surge.

After 100,000 seconds, the bottleneck created by the melt at the top of the soil region creates a critical block to vapor release. Interestingly, the pressure curves are not affected by the soil's initial liquid saturation. The history of the melt movement for case 3 (not shown) differs very slightly from that for case 4. The similarity in the two cases' melt growth can be explained in terms of the vapor history in the porous soil. Once a dry zone is established near the interface, the heat leaving the interface is not affected by the soil's overall saturation levels, therefore, the net heat entering the interface and consequent interface growth is the same for both cases.

The interface growth for case 5, depicted in figure 5, is increased because of the higher melt boundary temperature. This higher growth rate for case 5 causes the earlier development of a bottleneck accompanied by an earlier pressure rise as illustrated in figure 3.

CONCLUSIONS AND RECOMMENDATIONS

1. Coupling the three models to simulate the heat and mass transfer in the native soil adjacent to a growing melt yields some useful insights into the pressure history of the native soil. The basic model described in this paper could be enhanced to provide accurate simulations the ISV process.
2. The initial liquid saturation level was not found to have much affect on melt growth.
3. Higher melt growth rates are clearly associated with earlier MEE's.
4. Including the effect of density differences between the melt and the native soil would require a more sophisticated model but would yield better accuracy.
5. Properties for the melt are highly temperature dependent. Including temperature-dependent properties would affect the melt growth rate and, consequently, the native soil's pressure history.

REFERENCES

Karki, K. C. and H. C. Mongia, 1990, "Evaluation of a coupled solution approach for fluid flow and scalar transport in body-fitted coordinates", *Int. J. Numer. Methods in Fluids*, vol. 11, pp 1 - 20.

Kuo, C. H., 1994, "A Computational Study of Phase-Change Problems Using an Adaptive Grid in the Front-Tracking Method", Ph.D. Dissertation.

Kuo, C. H. and W. C. Schreiber, 1994, "An interface-tracking method for solving pure substance phase-change problems using nonsteady curvilinear coordinates", *Current Developments in Numerical Simulation of Flow and Heat Transfer* (HTD-vol. 275), pp. 57 - 64, Ed. K. Vafai and J. L. S. Chen.

Pruess, K. and T. N. Narasimhan, 1985, "A practical method for modeling fluid and heat flow in fractured porous media", *Society of Petroleum Engineers Journal*, vol. 25, pp 14 - 26.

Pruess, K., 1986, *TOUGH User's Guide*, Sandia National Laboratories research report (NUREG/CR-4645, SAND 86-7104, RW)

Roberts, J. S., S. L. Woosley, D. L. Lessor, and C. Strachan. 1992. Preliminary investigation for the potential for transient vapor release events during in situ vitrification based on thermal-hydraulic modeling, PNL-8170, Pacific Northwest National Laboratory, Richland, Washington.

Schreiber, W. C., 1996a, "A computer model for predicting two-phase ground water transport in the soil surrounding a growing melt in the *In Situ Vitrification* process", ASME Procedings of the 31st National Heat Transfer Conference (HTD-vol. 331), pp. 63-70, Ed. H. A. Hadim et al.

Schreiber, W. C., P. S. Lowery, and J. S. Roberts, 1996b, "A parameter study of the two-phase ground water transport in the soil surrounding a growing hemispherical In Situ Vitrification melt, HTD-vol 335, pp. 75-81, International Congress and Exposition (IMECE), Atlanta GA.

Thompson, J. F., Z. U. A. Warsi, and C. W. Mastin, 1985, *Numerical Grid Generation: Foundations and Applications*, North-Holland, New York.